Proc. Natl. Acad. Sci. USA
Vol. 94, pp. 879–883, February 1997
Cell Biology

Cell–cell contact changes the dynamics of lamellar activity in nontransformed epitheliocytes but not in their *ras*-transformed descendants

(neoplastic transformation/actin cytoskeleton/cell adhesion/contact inhibition of movement)

N. A. GLOUSHANKOVA*, N. A. ALIEVA†, M. F. KRENDEL‡, E. M. BONDER‡§¶, H. H. FEDER¶, J. M. VASILIEV*†, AND I. M. GELFAND†¶

‡Program in Cellular and Molecular Biodynamics, and ¶Department of Biological Sciences, Rutgers University, 101 Warren Street, Newark, NJ 07102; and *Oncological Scientific Center of Russia and †Belozersky Institute of Physico-Chemical Biology, Moscow State University, Moscow, 115522, Russia

Contributed by I. M. Gelfand, November 22, 1996

ABSTRACT **We investigated the structural and functional alterations of active lamellae during initial cell–cell collision and establishment of cell–cell contacts in wounded cultures of nontransformed rat epitheliocytes (IAR-2 line) and their *ras*-transformed descendants (C4 line). Typically, the leading edges of nontransformed cells formed multiple transient contacts followed by establishment of small, stable contacts that would undergo lateral expansion. Formation and expansion of the contact area was accompanied by accumulation of the cell–cell adhesion molecules E-cadherin, β-catenin, and plakoglobin. During lateral expansion, the circumferential bundles of actin filaments, characteristic of IAR-2 cells, disassembled at the site of stable contact forming a concave arc-like actin bundle between adjacent cells at the expanding edge. Pseudopodial activity was completely inhibited in the contact zone and partially inhibited at the free lamellar edges adjacent to the zone of contact. Con A-coated beads on the plasma membrane at the zone of contact stopped undergoing centripetal transport but now moved along the cell–cell boundary. On the other hand, *ras*-transformed cells developed overlapping lamellae and exhibited no detectable change in activity of lamellae, localization of adhesion molecules, and organization of the actin cytoskeleton. We propose that contact-induced reorganization of cell surface adhesion molecules and the underlying cortical cytoskeleton leads to development of lateral traction that may be an essential element in inducing expansion of the contact and in inhibiting local pseudopodial activity.**

Essential steps in organizing cultured tissue cells into tissue-like, multicellular epithelial islands and sheets are modifications of motile activity and formation of cell–cell contacts. Nearly two decades ago, the seminal studies of Abercrombie (1) and colleagues established that collisions by the leading edges of motile nontransformed fibroblasts and epitheliocytes induced "paralysis" of pseudopodial activity and inhibition of forward translocation, the so-called contact inhibition of movement. It was suggested that the basic invasive characteristics of malignant cells may, in part, be attributed to defects in the cell's ability to undergo contact inhibition (2).

While contact inhibition of movement is a well known phenomenon, the cellular mechanisms underlying this activity remain unknown. The aim of the present report is to provide an analysis of cell–cell contact formation by correlating dynamics of lamellar motility, structural reorganization of the actin cytoskeleton, and localization of cell adhesion molecules in nontransformed epitheliocytes (IAR-2 cells) and their *ras*-transformed descendants (C4 cells). Cell–cell collisions of IAR-2 cells resulted in dramatic modification of lamellar dynamics as determined by observations of surface bead motility and quantitative analysis of pseudopodial activity. Correlated with the observed changes was an accompanying reorganization of the underlying cortical actin cytoskeleton and concentrated localization of cell adhesion molecules. By contrast, cultures of *ras*-transformed epitheliocytes did not exhibit detectable modifications in lamellar dynamics, bead motility, adhesion protein localization, and actin organization. These observations suggest that contact inhibition of cell movement and cell–cell contact expansion are driven by directional changes in mechanical tension resulting from reorganization of the cortical actin cytoskeleton.

MATERIALS AND METHODS

Cell Culture and Light Microscopy. Rat liver epithelial cell line, IAR-2, and their *ras*-transformants, C4 cells, were obtained (3, 4) and cultured as described (5). Cells were plated onto glass coverslips, cultured to confluency, and scraped with a hypodermic needle to create a narrow wound. After wounding, the cultures were incubated for 3–4 h before further experimentation. High resolution differential interference contrast (DIC) microscopy was carried out on a Zeiss Axiophot microscope equipped with a Plan-Neofluar ×100 (NA 1.3), DIC optics, and an air curtain temperature-controlled stage that maintained sealed cultures at 33°C. Images were collected using a Hamamatsu Newvicon camera (Hamamatsu, Middlesex, NJ) and the resultant images were stored onto S-VHS videotape. In some experiments, video images were averaged for 8 frames using a Quantex image processor before videotaping

Analysis of Lamellar Activity. Pseudopodial activity was quantitated as described (5). Briefly, the outlines of cell edges were obtained using two still video frames separated by a 20-sec time interval, the outlined images were merged, and pseudopodial activity was quantitated by dividing the total area of protrusion or retraction by the length of the active edge of the cell. Motility of Con A-coated beads attached to lamellar surfaces was measured as described in Gloushankova *et al.* (5). Beads were positioned onto the plasma membrane in the region of cell–cell contact using a laser optical tweezers and bead movement was recorded onto S-VHS videotape. Occasionally, observations of bead motility were performed using beads that spontaneously attached to the lamellar surface. Rates and trajectories of bead translocation were determined by tracking the position of beads at 1-min intervals using National Institutes of Health IMAGE Version 1.44 software.

The publication costs of this article were defrayed in part by page charge payment. This article must therefore be hereby marked "*advertisement*" in accordance with 18 U.S.C. §1734 solely to indicate this fact.

0027-8424/97/94879-5$2.00/0
PNAS is available online at **http://www.pnas.org**.

§To whom reprint requests should be addressed.

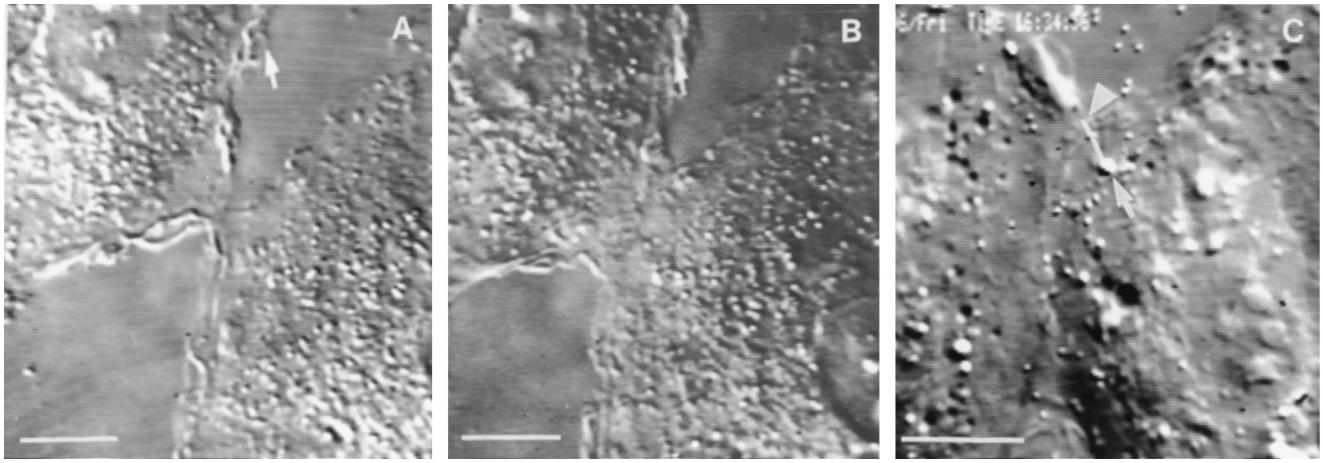

FIG. 1. Video micrographs of colliding IAR-2 cells. (*A*) Formation of an initial stable contact between IAR-2 cells. The arrow shows a lamelipodium at the free cell edge. (*B*) Expansion of the contact shown in *A* after 20 min. (*C*) Con A–bead translocation on the surface of an IAR-2 cell in the region of a new cell–cell contact. The white line shows the path the bead (see arrow) followed over the first 5 min after attachment to the cell surface; an arrowhead points to the bead's final position after 5 min. The bead was moving along the cell–cell boundary toward the free edge of the contact. (Bar = 10 μm.)

Fluorescence Microscopy. Cells cultured on coverslips were rinsed with PBS containing 1 mM $CaCl_2$ and then fixed by immersion into a 1:1 mixture of acetone/methanol for 10 min at −20°C. After fixation, the coverslips were incubated for 10 min in PBS containing 0.2% BSA followed by probing with mAbs raised against E-cadherin, β-catenin (Transduction Laboratories, Lexington, KY), plakoglobin (PG5.1), or desmoglein (Dg3.10) (generously provided by S. M. Troyanovsky, Washington University Medical School). After incubation in primary antibodies, coverslips were incubated in fluorescein isothiocyanate (FITC)-conjugated goat anti-mouse secondary antibodies. For fluorescence localization of actin and vinculin, cells were rinsed with PBS, fixed in PBS containing 3.7% formaldehyde, and permeabilized by a 3-min incubation in 1% Triton X-100 in PBS. Next, cells were incubated in rhodamine–phalloidin (Molecular Probes) and anti-vinculin mAbs (VIN-1-15; Sigma) for labeling of actin and vinculin, respectively. Anti-vinculin antibodies were localized using a FITC-labeled secondary antibody. Fluorescence images were collected using the Bio-Rad MRC 1000 laser scanning confocal microscope system mounted onto Nikon optics. In some experiments, conventional epifluorescence images were collected using a Leitz Aristoplan microscope.

RESULTS

Video Light Microscopic Analysis of Lamellar Dynamics During Cell–Cell Contact Formation by IAR-2 Cells. As IAR-2 cells migrated into the wound the free edges of cells began forming cell–cell contacts. There were three distinct stages during the process of forming stable cell–cell contacts. Initially, cells formed "transient contacts" during repeated collisions of leading edges resulting from rapid protrusion and retraction of lamellipodia. Cells were observed to remain in the transient contact stage for 1–10 min. During repeated collision and retraction events, there would occur incomplete retraction of lamellipodia resulting in formation of a 2- to 3-μm-wide "initial stable contact" (Fig. 1*A*). After formation of the initial stable contact there was decreased protrusive activity in the proximity of the area of stable contact and only a limited degree of overlapping of the adjoining lamella; maximal overlap was 8.66 ± 2.99 μm^2 during the 10-min period after formation of the initial stable contact. Next, the contact began "lateral expansion" by bidirectional outward spreading of the edge of the contact (Fig. 1*B*). The free edges of the lamellae on either side of the expanding contact acquired smooth contours and they exhibited significantly lower rates of protrusive activity as compared with lamellar activity before contact (Table 1).

To further assess the effect of contact formation on lamellar activity, Con A-coated beads were placed upon the surface of active edges of cells migrating into a wound. Before formation of initial stable contacts, Con A-coated beads exhibited typical centripetal directed motility as described (5). Beads on the surface near the lateral edge of an expanding contact tended to move tangentially toward the edge at an average velocity of 0.51 ± 0.08 μm/min while the edge of the cell was undergoing expansion at a velocity of 0.87 ± 0.15 μm/min (Fig. 1*C*). The difference between the rate of bead movement and the rate of lateral expansion resulted in increased separation between the bead and the edge of the cell. Once cells formed fully stable contacts, as in established sheets of cells, there was no significant movement of beads placed on the upper surface of the cell.

Analysis of the Actin Cytoskeleton and Cell Adhesion Molecules in IAR-2 Cells. IAR-2 cells were found to typically have a distinct circumferential bundle of actin filaments immediately behind the free edges of lamellae while straight, thin bundles of filaments were observed in the central regions of the cells (Fig. 2*A*). Indirect immunofluorescence labeling with anti-vinculin antibodies detected the presence of numerous focal adhesions (Fig. 3*A*) that were typically observed under circumferential bundles of actin and at the ends of the straight bundles of actin filaments. In cells having formed initial stable contacts, the circumferential bundles of actin filaments became discontinuous in the area of cell–cell contact and there now appeared thin filament bundles or filaments oriented radially in the area of cell–cell contact (Fig. 2*B*). In late stage contacts, circumferential bundles were no longer observed in the zone of contact but instead the bundles terminated at the site of lateral expansion of the contact (Fig. 2*C*). Thus termination of the bundles of actin filaments in adjoining cells resulted in formation of a concave, arc-like span of actin filaments along the sides of the expanding contact. Within the zone of contact, rhodamine–phalloidin staining identified the presence of filaments or bundles of filaments

Table 1. Mean rates (μm/min ± SEM) of protrusion and retraction of lamellipodia at the active edges of nontransformed IAR-2 cells and *ras*-transformed C4 cells before and after cell–cell contact

	Before contact		After contact	
Cell type	Protrusion	Retraction	Protrusion	Retraction
IAR-2	0.78 ± 0.12	0.66 ± 0.10	0.42 ± 0.07	0.25 ± 0.07
C4	1.08 ± 0.18	1.20 ± 0.20	1.43 ± 0.28	0.84 ± 0.18

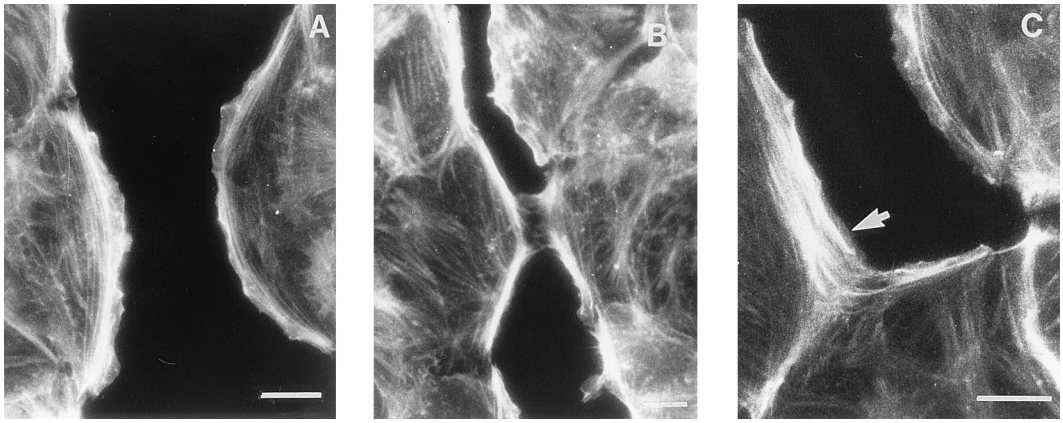

FIG. 2. Reorganization of actin filaments in IAR-2 cells during formation of a new cell–cell contact. Shown are conventional epifluorescence micrographs of cells stained with the actin filament-specific probe, rhodamine–phalloidin. (*A*) Free edges of wounded IAR-2 monolayers contained prominent marginal bundles of actin filaments. (*B*) As an initial stable contact formed, marginal actin bundles at the site of the contact began to disassemble. (*C*) A concave arc-like bundle of actin filaments (arrow) was formed at the edge of the expanding contact. (Bar = 10 μm.)

oriented along and at oblique angles to the contact. Interestingly, in these zones, anti-vinculin antibodies stained focal contacts that were aligned along the long axis of the cell–cell contact (Fig. 3*B*).

To investigate the role of cell–cell adhesion molecules, IAR-2 cells were probed with anti-E-cadherin, anti-β-catenin, anti-plakoglobin, and anti-desmoglein antibodies during the process of cell–cell contact formation. In non-wounded regions of monolayers, E-cadherin and β-catenin were distinctly localized to a thin band running along the length of mature cell–cell contacts (Fig. 4). The free edges of cells did not exhibit any detectable localization of E-cadherin (Fig. 4 *A–C*) while occasionally β-catenin was detected at the free edge, at significantly lower levels than seen at cell–cell contacts (Fig. 4*D*). Observation of even the smallest cell–cell contact detected the presence of an enrichment of E-cadherin (Fig. 4 *A* and *B*) and β-catenin (Fig. 4*D*) at the sites of contact. Plakoglobin localization was essentially the same as observed for β-catenin whereas desmoglein was not detected at the free edges of cells but was localized to mature cell–cell contacts in cell monolayers (data not shown). As cell–cell contacts expanded, adhesion molecules continued to localize along the expanding edge (Fig. 4*C*). The observed enrichment of E-cadherin in early cell–cell contacts was not reported by McNeill *et al.* (6) for MDCK cells and may be a consequence of differences in the antibodies used in the two studies.

Video Light Microscopic Analysis of Lamellar Dynamics During Cell–Cell Contact Formation by C4 Cells. *ras*-transformed C4 cells did not exhibit any of the stages of cell–cell contact that were described for nontransformed IAR-2 cells. Typically, as the leading edges of cells collided in the wound there was no detectable change in lamellar activity as compared with that of the free edge of the cell (Table 1) and there was no observed formation of transient contacts. Consequently, there was mutual overlap of active lamellae (Fig. 5) resulting in an area of overlap that was up to 7 times larger (57.19 $\pm$ 13.91 μm^2) than the overlap seen in IAR-2 cells, during the first 10 min after initial cell–cell contact. As lamellar activity continued unabated, the region of overlap continued to spread as the free edges progressed forward into the wound. The absence of modification of lamellar activity was further substantiated by the observation that Con A-coated beads placed on the surface of an overlapping lamella continued to undergo centripetal translocation (Fig. 5*A*) at rates comparable to those measured for nonoverlapping lamellae (data not shown).

Analysis of Actin Cytoskeleton and Cell Adhesion Molecule Localization in C4 Cells. C4 cells did not possess circumferential bundles of actin filaments. In general, rhodamine–phalloidin staining identified the presence of thin, straight actin bundles that ran along the long axis of the cell as well as networks of short

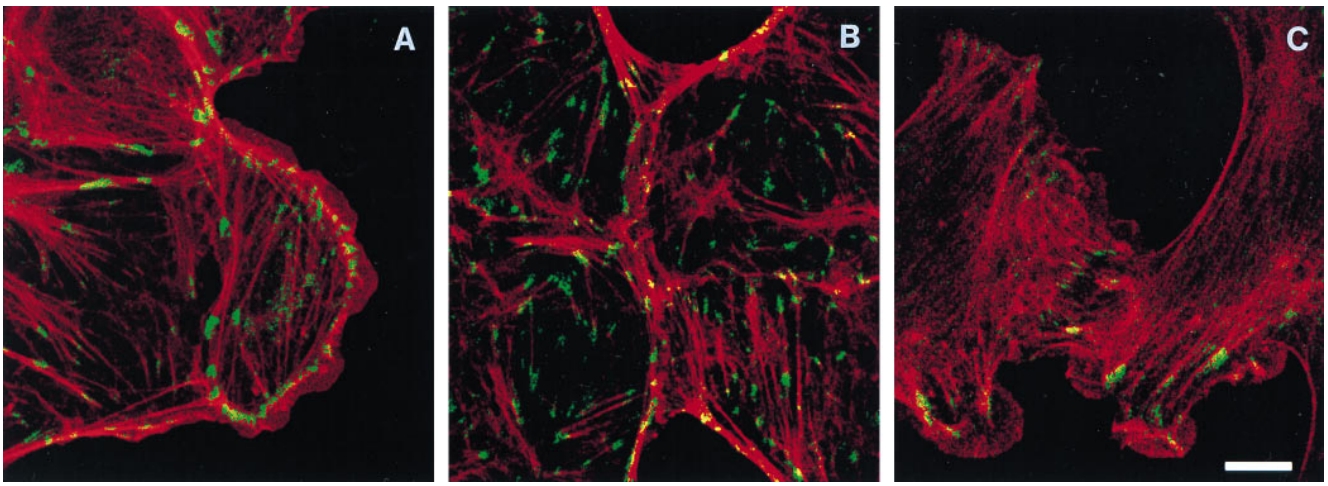

FIG. 3. Confocal images of IAR-2 and C4 cells double labeled for actin filaments (red) and vinculin (green). Areas where actin and vinculin staining overlapped are indicated by the yellow color. (*A*) Vinculin-positive focal adhesions at the free edge of a wounded IAR-2 cell monolayer did not have any preferential orientation relative to the cell edge. (*B*) A newly formed contact by four IAR-2 cells. Focal adhesions and straight actin bundles in the contact zone were oriented along the intercellular boundary. Note the concave actin arcs at the edges of the contact. (*C*) Overlapping C4 cells demonstrated a meshwork of actin filaments and orientation of focal adhesions along the cell axis. (Bar = 10 μm.)

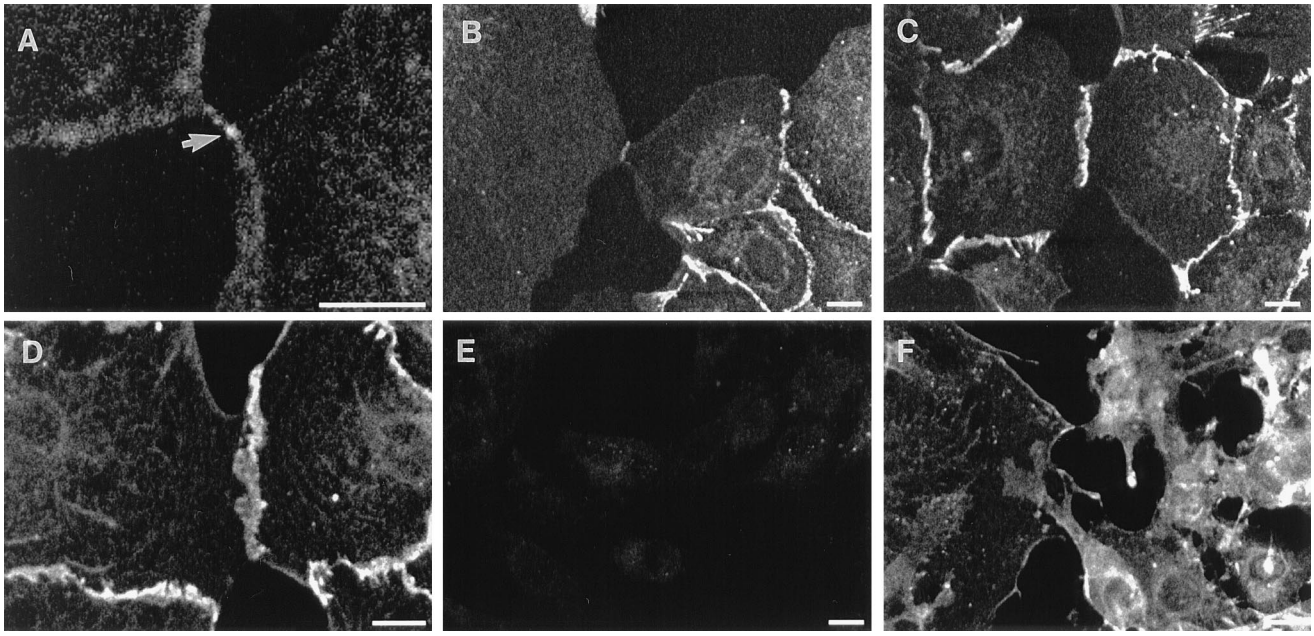

FIG. 4. Confocal images of indirect immunofluorescence staining of E-cadherin (*A–C* and *E*) and β-catenin (*D* and *F*). Accumulation of E-cadherin in the contact regions at different stages of contact formation and expansion in IAR-2 cells (*A–C*). Arrow indicates E-cadherin staining in an initial contact (*A*). Staining of IAR-2 cells for β-catenin showed accumulation of β-catenin in the contact zone (*D*). C4 cells did not exhibit significant staining for E-cadherin (*E*). β-Catenin in C4 cells was not enriched in the contact zone (*F*). (Bar = 10 μm.)

filaments within the active lamellae. As observed in IAR-2 cells, anti-vinculin antibodies localized the presence of vinculin at the ends of actin bundles (Fig. 3*C*). There was no discernible change in the organization of the actin cytoskeleton in C4 cells either during initial cell–cell contact or after the cells started to exhibit overlapping lamellae (Figs. 3*C* and 5*B*).

Anti-E-cadherin antibody staining resulted in little detectable staining relative to the levels of staining seen in IAR-2 cells (Fig. 4*E*); this was confirmed by the absence of detectable levels of E-cadherin by immunoblots of C4 cells (data not shown). Indirect immunofluorescence staining with anti-β-catenin antibodies resulted in diffuse cytoplasmic staining equivalent to the cytoplasmic staining observed in IAR-2 cells (Fig. 4*F*). There appeared to be a slight enrichment of β-catenin at some free edges (Fig. 4*F*); however, the enhanced level of staining was significantly lower than β-catenin levels observed at cell–cell contacts between IAR-2 cells. In regions where C4 cells were making contact or were overlapping there was no enhancement of β-catenin levels.

DISCUSSION

Nontransformed IAR-2 cells progress through three morphologically distinct stages during formation of stable cell–cell contacts, namely, repeated formation of transient contacts, formation of initial stable contact, and lateral expansion of initial stable contact. Previously, McNeill *et al.* (6) reported a similar three stage progression in the formation of cell–cell contacts by MDCK cells, and we now extend those observations to include detailed analyses of lamellar activity and associated changes in actin organization and cell adhesion molecule localization. Formation of initial transient contacts appears to be a consequence of protrusion and retraction of the lamellar edge. Upon formation of an initial stable contact there is a correlated quiescence of lamellar activity both at the site of contact and at lamellar edges lateral to the contact. This quiescence suggests the triggering of a cytoplasmic event, possibly a receptor-mediated signaling pathway (7, 8), that alters cytoskeletal activity from one driving cell translocation to one facilitating formation of cell–cell contact. Quiescence

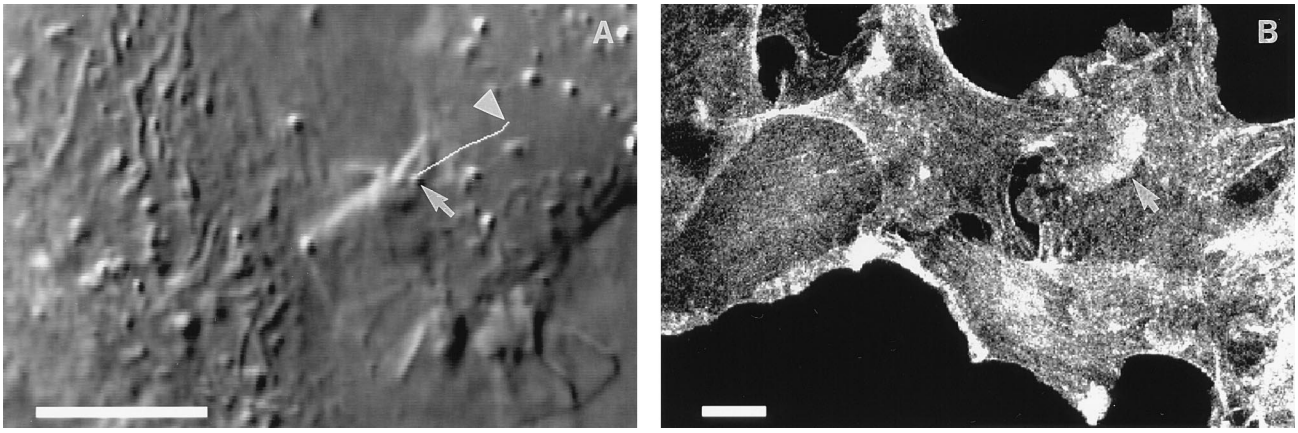

FIG. 5. Dynamics of collision events in C4 cells. (*A*) Con A-coated bead movement on the surface of a C4 cell overlapping with another cell. Bead trajectory over the first 5 min after bead attachment is indicated by the white line. The bead (see arrow) moved centripetally along the cell axis; the arrowhead points to the location of the bead after 5 min. (*B*) Actin staining of overlapping C4 cells in a narrow wound imaged using confocal microscopy. An actin-rich lamella of one of the overlapping cells is shown by an arrow. (Bar = 10 μm.)

of lamellar activity was also observed when beads placed onto the zone of contact were no longer transported centripetally. Instead beads moved laterally along with the zone of expansion, albeit slower, and eventually stopped moving while the edge continued to expand. By contrast, the dynamics of pseudopodial activity and centripetal bead motility remained essentially unchanged after C4 cells make contact, suggesting that *ras*-transformation altered the cells ability to respond to the presence of another cell.

The observed alteration of lamellar activity in IAR-2 cells was well correlated with structural reorganization of the actin cytoskeleton and localization of cell adhesion molecules. In cells possessing initial stable contacts, the circumferential bundle of filaments were disassembled in the area of the contact and the newly formed ends of the bundles were observed to "insert" into the advancing edge of the expanding contact (see Fig. 6). The remaining segments of circumferential bundles in adjoining cells now formed two concave arc-like bundles of filaments positioned at the expanding edges of the cell–cell contact. Coincident with the breakdown of the circumferential bundles of filaments at the contact zone was the formation of thin bundles of actin filaments that were oriented obliquely to and along the axis of expansion. Interestingly, as the contacts became larger, vinculin staining detected that the focal adhesions were lying along the axis of expansion. There were no observed changes in the actin cytoskeleton of C4 cells that were in the process of making contact or possessing overlapping lamellae.

The cell adhesion molecules E-cadherin, β-catenin, and plakoglobin became enriched at the site of an initial stable contact and continued to be concentrated to the site during contact expansion. Thus, localized enrichment of E-cadherin and its associated proteins, β-catenin and plakoglobin, could participate in expansion of the cell–cell contact by "cadherin zippering" (9). Additionally, the localization of E-cadherin, β-catenin, and plakoglobin at initial stable contacts may promote a cell signaling event (7, 8) that in turn triggers cytoskeletal reorganization and modifies lamellar activity. Decreases in protrusive activity and loss of centripetal flow of surface receptors in and about the site of cell–cell contact would provide for greater opportunity for E-cadherin dimerization and subsequent zippering. Lateral movement of Con A-coated beads in the expanding area of cell–cell contact suggests receptor movement along the axis of expansion, further facilitating cadherin positioning along the contact. Enrichment of E-cadherin at the site of contact would then serve in targeting of β-catenin and plakoglobin to the contact site where they function in producing stable cytoskeletal interactions. The apparent absence of E-cadherin in C4 suggests that these cells are deficient in cell–cell recognition activity that is required for subsequent reorganization of the cytoskeleton during contact inhibition of movement. Alternatively, *ras* expression may access other aspects of cell adhesion, as reported for *ras*-transformed MCF-10A human breast epithelial cells that express E-cadherin but demonstrate elevated β-catenin phosphorylation and decreased association of β-catenin with the actin cytoskeleton (10).

Our observations on the dynamics of lamellar activity, localization of adhesion molecules, and reorganization of the actin cytoskeleton provide insight into the potential mechanism underlying expansion of cell–cell contacts. IAR-2 cells have prominent circumferential bundles of actin filaments as well as numerous stress fibers that could participate in mechano-chemical force production (11). Tension acting along the circumferential bundle of filaments (Fig. 6*A*, small arrows) produces an axial force (Fig. 6*A*, large arrows) driving centripetal flow of membrane receptors. During contact formation, the circumferential bundles of actin filaments in both cells begin to dissociate resulting in a discontinuity that leads to tangential tension acting along the edge of the cell on both sides of the contact (Fig. 6*B*, small arrows). The sum of the tensions from both cells results in an outward force (Fig. 6*B*, large arrows) that acts to stretch and expand the contact. Mechanistically, this process is similar to the "purse string" contraction of annular actin cables that participate in wound closure in embryo epidermis (12) and in cultured epithelial sheets (13). The tangential forces would also tend to align filaments along the direction of tension, as observed in the zone of cell–cell contact, thereby decreasing pseudopodial activity (14).

In conclusion, coordinated changes in the location of cell adhesion molecules, organization of the actin cytoskeleton, and in spatial dynamics of lamellae appear to be essential for cell–cell contact formation and contact inhibition of movement. Deficiencies in modulation of these activities may be partially responsible for the aberrant behavior of oncogene-transformed cells.

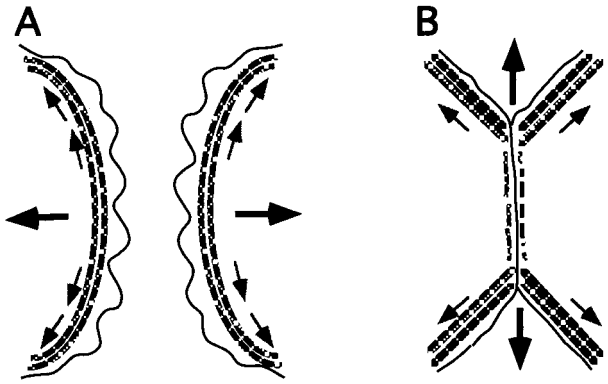

FIG. 6. Model for orientation of traction forces driving contact expansion. (*A*) Actin organization and force diagram before formation of cell–cell contact. (*B*) Actin organization and force diagram during cell–cell contact expansion. Stippled lines represent the circumferential bundles of actin filaments, small arrows illustrate the direction of tension along actin filaments, and large arrows show the vectorial sum of tensional forces (see *Discussion* for details).

We gratefully thank Dr. S. M. Troyanovsky (Washington University Medical School) for helpful discussions and gifts of antibody reagents and Mr. V. Sirotkin (Rutgers University) for constant interest and input. This work was supported by the Gabriella and Paul Rosenbaum Foundation (to I.M.G.), an International Science Foundation Grant and Russian Foundation of Basic Investigations Grant (to J.M.V.), and an American Heart Association–NJ Affiliate Grant and the Charles and Johanna Busch Memorial Fund (to E.M.B.).

1. Abercrombie, M. (1970) *In Vitro* **6,** 128–142.
2. Vasiliev, J. M. & Gelfand, I. M. (1981) *Normal and Neoplastic Cells in Culture* (Cambridge Univ. Press, Cambridge, U.K.).
3. Montesano, R., Saint-Vincent, L., Drevon, C. & Tomatis, L. (1975) *Int. J. Cancer* **16,** 550–558.
4. Gloushankova, N. A., Lyubimova, A. V., Tint, I. S., Feder, H. H., Vasiliev, J. M. & Gelfand, I. M. (1994) *Proc. Natl. Acad. Sci. USA* **91,** 719–722.
5. Gloushankova, N. A., Krendel, M. F., Sirotkin, V. A., Bonder, E. M., Feder, H. H., Vasiliev, J. M. & Gelfand, I. M. (1995) *Proc. Natl. Acad. Sci. USA* **92,** 5322–5325.
6. McNeill, H., Ryan, T. K., Smith, S. & Nelson, W. J. (1993) *J. Cell Biol.* **120,** 1217–1226.
7. Geiger, B. & Ayalon, O. (1992) *Annu. Rev. Cell Biol.* **8,** 307–332.
8. Gumbiner, B. M. (1996) *Cell* **84,** 345–357.
9. Klymkovsky, M. W. & Parr, B. (1995) *Cell* **83,** 5–8.
10. Kinch, M. S., Clark, G. J., Der, C. J. & Burridge, K. (1995) *J. Cell Biol.* **130,** 461–471.
11. Mitchison, T. J. & Cramer, L. P. (1996) *Cell* **84,** 371–379.
12. Martin, P. & Lewis, J. (1992) *Nature (London)* **360,** 179–183.
13. Bement, W. M., Forscher, P. & Mooseker, M. S. (1993) *J. Cell Biol.* **121,** 565–578.
14. Kolega, J. (1986) *J. Cell Biol.* **102,** 1400–1411.